

Low-temperature synthesized aluminosilicate glasses

Part IV *Modulated DSC study on the effect of particle size of metakaolinite on the production of inorganic polymer glasses*

H. RAHIER^{*§}, J. F. DENAYER[‡], B. VAN MELE^{*}

^{*}Department of Physical Chemistry and Polymer Science, [‡]Department of Chemical Engineering, Vrije Universiteit Brussel, Pleinlaan 2, B-1050 Brussels, Belgium
E-mail: hrahier@vub.ac.be

The effect of the particle size of metakaolinite on the reaction kinetics of low-temperature synthesized inorganic polymer glasses is studied. The heat capacity of the material during isothermal cure is measured by Modulated DSC (MDSC). This signal can be followed quantitatively during the complete course of the reaction, whereas the heat flow signal is sometimes too small for quantitative interpretations. A characteristic time for the reaction, defined as onset of vitrification, is also measured with Dynamic Mechanical Analysis (DMA). The DMA and MDSC results show that the reaction rate increases with decreasing particle size of metakaolinite, at least till a particle size of about 2 μm . It can be concluded that the first step of the reaction, breaking down the metakaolinite grains, occurs at the surface of the particles. The second step is the building of a network starting from the reaction products of the former reaction. © 2003 Kluwer Academic Publishers

1. Introduction

The Low-Temperature synthesized Inorganic Polymer Glasses (IPG) characterized in this work are amorphous inorganic polymers formed at room temperature by the heterogeneous reaction of a two component system (solid/liquid) [1–6]. The raw materials for IPG are a powdered dehydroxylated clay mineral (metakaolinite, Mk) and an aqueous sodium or potassium silicate solution. During the exothermic polymerization of metakaolinite with the silicate solution a three dimensional aluminosilicate network is formed (IPG). In previous work was shown that this reaction can be studied with Modulated Differential Scanning Calorimetry (MDSC) and Dynamic Mechanical Analysis (DMA) [1, 2]. The influence of the composition of the raw materials on the chemical short range order of IPG was investigated with Fourier Transform Infrared (FTIR) and Magic Angle Spinning NMR (MAS NMR) spectroscopy [3, 6].

NMR can also be used to elucidate the nature of the species in the silicate solution [7, 8]. Besides the hydroxyl ion, the silicate solution contains the $\text{Si}(\text{OH})_4$ monomer and several types of related oligomers, such as the dimer, trimer and so on. The relative amounts of the different species depend on the $\text{SiO}_2/\text{Na}_2\text{O}$ and $\text{H}_2\text{O}/\text{Na}_2\text{O}$ ratios.

Preliminary MDSC results show an influence of the specific surface of the solid phase (Mk) on the reac-

tion kinetics of this heterogeneous synthesis of IPG [5]. In this paper, the influence of the particle size on the isothermal reaction kinetics will be studied in more detail. For this purpose, additional MDSC experiments will be compared with DMA results. Some preliminary and general insights on the more detailed heterogeneous reaction mechanism will be deduced.

2. Experimental

2.1. Raw materials

Metakaolinite ($\text{Al}_2\text{O}_3 \cdot 2\text{SiO}_2$) was obtained by heating kaolinite (KGa-1 from Source Clay Minerals Repository, University of Missouri, Columbia) during 1 h at 600°C. To obtain the different particle size distributions, Mk was fractionated by sedimentation in water (see [5] and 2.2.3). The silicate solution was $\text{Na}_2\text{O} \cdot 1.4\text{SiO}_2 \cdot 10\text{H}_2\text{O}$. More details on the materials used are described in [1].

2.2. Techniques

2.2.1. Modulated differential scanning calorimetry (MDSC)

2.2.1.1. Theory [9]. In MDSC a sample is subjected to a modulated temperature program obtained by superimposing a sine wave to the conventional isothermal or

[§]Author to whom all correspondence should be addressed.

linearly changing temperature program

$$T = T_0 + \beta \cdot t + A_T \cdot \sin(\omega t)$$

where T is the temperature, T_0 is the initial temperature, β is the heating rate in K/s , ω is the modulation angular frequency in s^{-1} , and t is the time. This modulated temperature input gives rise to a modulated heat flow response which consists of an underlying and a cyclic heat flow signal. Assuming that the temperature modulation is small so that over the temperature interval of one period the response of the rate of the kinetic processes to the temperature can be estimated as linear, the heat flow response can be written as

$$\begin{aligned} dQ/dt = & Cp(\beta + A_T \cdot \omega \cos(\omega t)) \\ & + f(t, T) + A_k \cdot \sin(\omega t) \end{aligned}$$

where Q in J is the amount of heat transferred to the sample, $f(t, T)$ in W is the average response of a kinetic phenomenon to the underlying temperature program and A_k in W is the amplitude of the kinetic response to the temperature modulation. In reality a phase shift will exist between the imposed temperature program and the measured heat flow. If this phase shift is small, as is the case in the experiments described in this paper, the following 'simple deconvolution' of the signals can be performed.

The underlying signals for both temperature and heat flow are calculated by an averaging process that subtracts the effects of the perturbation. The resulting underlying or total heat flow and the underlying temperature reconstitute quantitatively the thermoanalytical curve measured by conventional DSC. Using a discrete Fourier transform algorithm, the cyclic component of both temperature input and heat flow response is extracted. Comparison of the amplitude of the cyclic heat flow, A_{HF} , with the amplitude of the heating rate, $A_T \cdot \omega$, results in an additional signal: the 'cyclic' or complex heat capacity Cp

$$Cp = A_{HF}/(A_T \cdot \omega)$$

Multiplying the heat capacity by minus the underlying heating rate gives the 'reversing' heat flow, HF_R

$$HF_R = -Cp \cdot \beta$$

The non reversing heat flow, HF_{NR} , is the difference between the total heat flow and the reversing heat flow

$$HF_{NR} = HF_{tot} - HF_R$$

MDSC offers several advantages over conventional DSC, such as the disentanglement of overlapping phenomena, the measurement of heat capacity during quasi-isothermal experiments and the measurement of weak signals [10–13].

2.2.1.2. Experimental. Isothermal and non-isothermal measurements were performed on a DSC 2920 of TA Instruments, equipped with a temperature modulation

MDSC™ option and a refrigerated cooling system (RCS). The purge gas was He. Reusable high pressure stainless steel sample pans (PerkinElmer) were taken. The sample (about 30 mg) was heated as fast as possible (temperature jump) from 20°C to the isothermal temperature (35°C). A period of 100 s and amplitude of 0.5°C were chosen. Temperature calibration was done with cyclohexane and indium. The latter was also used for enthalpy calibration. Heat capacity was calibrated quasi-isothermally with water at 35°C.

2.2.2. Dynamic mechanical analysis

The DMA 7 of Perkin Elmer was used with a quartz expansion probe (diameter 1 mm). The purge gas was He. The applied frequency in all DMA measurements was 1 Hz. The reaction mixture was poured in a cylindrical container and covered at the surface with a thin rubber seal (see [2] for a complete description of this experimental set-up). The samples were placed in the preheated furnace (35°C).

2.2.3. Particle size analysis and specific surface

The surface area of Mk (as received) and of Mk fractions obtained by sedimentation was determined with nitrogen porosimetry. Prior to the experiments, the samples were outgassed at room temperature under a vacuum of 10^{-5} Torr. When a sufficient grade of vacuum was attained, the temperature was increased at 0.5°C per minute to 450°C. The samples were kept during 10 h at this final temperature. After the pretreatment procedure, nitrogen adsorption isotherms at 77 K were determined using a Fisons Sorptomatic 1990 device. All experimental isotherms were found to give a Type II nitrogen adsorption isotherm (according to the IUPAC 1985 classification), indicating the formation of an adsorbed layer whose thickness increases progressively with increasing pressure. This isotherm is typically obtained with non-porous materials, such as the investigated metakaolinite samples.

The surface area was calculated from the experimental isotherms using the B.E.T. method [14]. Data points obtained in the relative pressure range between 0.05 and 0.33 (typically, about 10 points) were used in the BET surface area calculation.

The particle size distribution was measured in water with a coulter LS130. Ultrasonic vibration to separate the Mk particles was used previous to recording the spectra. The particle size distribution was calculated using a Fraunhofer optical model. More details were published in [5].

3. Results and discussion

To study the influence of the particle size of the solid reaction component on the kinetics of the low-temperature production of IPG, metakaolinite, Mk, was first fractionated by a sedimentation procedure.

The particle size distribution of Mk (as received), and of some Mk fractions after sedimentation are shown in Fig. 1 and listed in Table I.

TABLE I Median and variance of particle size distribution of Mk (as received) and other Mk fractions

Fraction	BET specific surface (m^2/g)	Median (μm)	Variance (μm^2)
0 (as received)	—	3.6	87
1	9	30	440
2	8.7	13	130
3	12.4	4.3	19
4	13.9	3.1	80
5	14.3	2.3	11
6	16.8	1.8	32
7	19.8	1.5	42

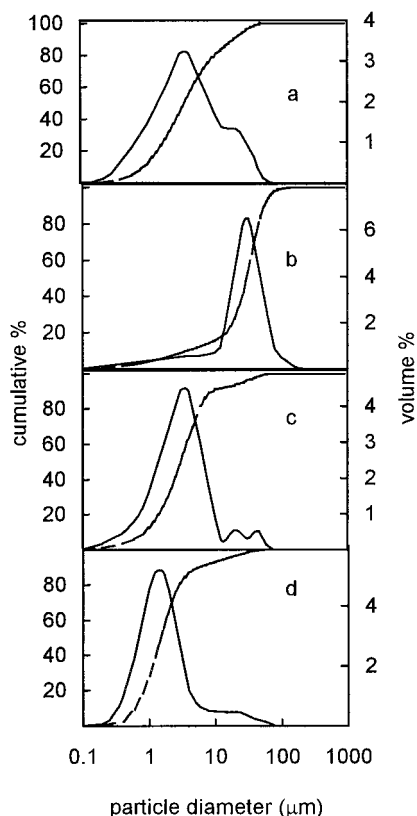


Figure 1 Particle size distribution of some Mk fractions of Table I: (a) Mk as received fraction 0, (b) fraction 1, (c) fraction 4, and (d) fraction 7.

The experimentally determined specific surface areas are given in Table I. Values between 8.7 and $22.7 \text{ m}^2/\text{g}$ were obtained. A value of $17 \text{ m}^2/\text{g}$ for a common kaolinite sample was found in literature [15], which is close to the average value found in this study ($14.7 \text{ m}^2/\text{g}$). If the particles are considered as composed of spherical particles characterized by a particle diameter equal to the median of the corresponding distribution a good correlation is found between the so calculated specific area and the measured specific area.

To study the influence of the particle size on the reaction rate, macroscopic techniques will be used here. For the complex reaction under study one should always bear in mind that the reaction rate changes with the conversion in a specific way. From each type of measurement reaction rates at a certain conversion can be deduced, enabling the comparison of the reaction rates between the different fractions. A more detailed study on the reaction kinetics and the reaction mechanism will be published elsewhere.

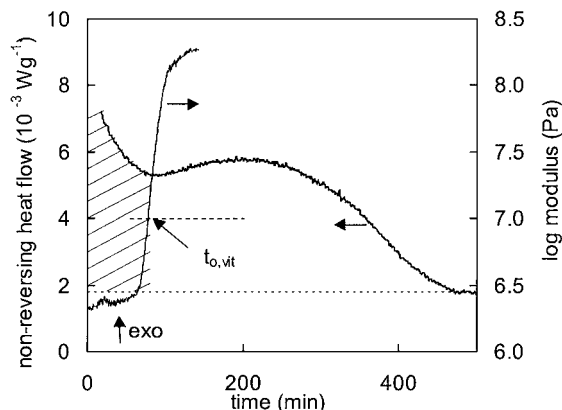


Figure 2 Storage modulus (DMA) and heat flow (MDSC) during isothermal cure at 35°C for Mk fraction 6 (see Table I). $t_{0,\text{vit}}$ (in min) is considered to characterize the onset of vitrification.

During the low-temperature exothermic reaction, the heterogeneous reaction mixture is vitrifying. The onset of the vitrification process (start of network formation) can be characterized by DMA [2]: due to the network formation, the storage modulus starts increasing after a certain reaction time. To be able to compare the reactivity of different systems, a characteristic time is defined as shown in Fig. 2: the onset of vitrification ($t_{0,\text{vit}}$), where the storage modulus of the reaction mixture reaches 10^7 Pa . At this stage the conversion derived from the DSC heat flow signal (shaded area in Fig. 2) is about 25% (see also [2]).

The onset of vitrification coincides with the onset of the decrease in heat capacity as measured by MDSC (see Fig. 3).

In contrast to most organic systems, the vitrification of the reacting system does not cause a sudden decrease in the reaction rate, which is proportional to the heat flow signal [2]. On the contrary, the reaction rate seems not to be influenced by the vitrification. Remark that the vitrification starts at relatively low conversions (at about 25% according to reaction heat, see also [2]).

The heat flow phase angle (Fig. 3) goes through a local minimum during the reaction and then reaches a constant value even somewhat earlier than the heat flow. It should be noted that the phase angle remains small during reaction (max. 0.02 rad). Similar curves were obtained for the other Mk fractions. Therefore in

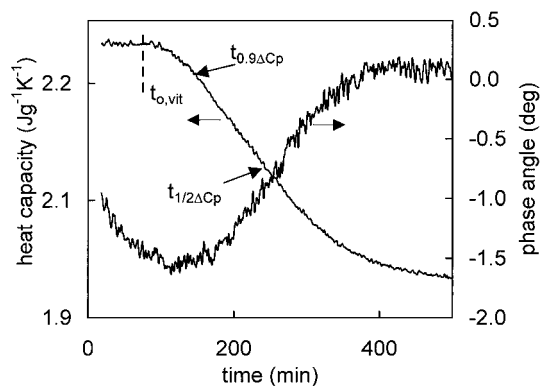


Figure 3 Heat capacity and heat flow phase angle (MDSC) during isothermal cure at 35°C for Mk fraction 6 (see Table I). The time at half the decrease in heat capacity is indicated as $t_{1/2\Delta C_p}$.

all cases a simple deconvolution will be sufficient. In organic thermosetting systems the local minimum is linked to a relaxation during vitrification. Fig. 3 shows that the phase angle decreases from the start of the reaction, thus the local minimum is not only linked to the vitrification (formation of solid phase) as observed from the decrease in the heat capacity. A plausible reason for this is that already from the beginning of the reaction a solid phase, Mk, is involved in the reaction.

Classically, the influence of the particle size on the reaction rate can be studied with the DSC heat flow signal (Fig. 4), which is proportional to the reaction rate.

Because of the low reaction rate at the chosen reaction temperature (35°C) the heat flow signal is weak and influenced to a large extent by baseline instabilities. To be able to use this signal quantitatively, experiments at a higher temperature (60°C) were performed (Fig. 4b). At this temperature, the reaction is however too fast to obtain a reliable heat capacity signal. The shape of the heat flow signal at both temperatures is comparable. It shows the complexity of the overall reaction which is most probably composed of different steps, each with its own reaction enthalpy and reaction rate. The maximum heat flow, thus maximum reaction rate occurs close to the beginning of the reaction and shifts to even shorter times for the smaller particles. For all fractions an autocatalytic effect is observed: the reaction rate increases after a certain time. For the smaller particles, this is preceded by a steadily decrease in reaction rate.

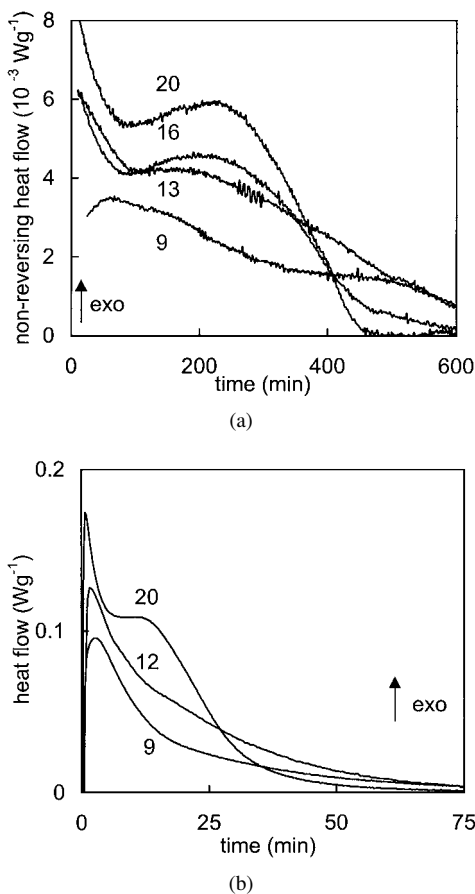


Figure 4 (a) Heat flow signals (DSC) during isothermal cure at 35°C for the different Mk fractions (specific surface indicated in m^2/g) and (b) at 60°C.

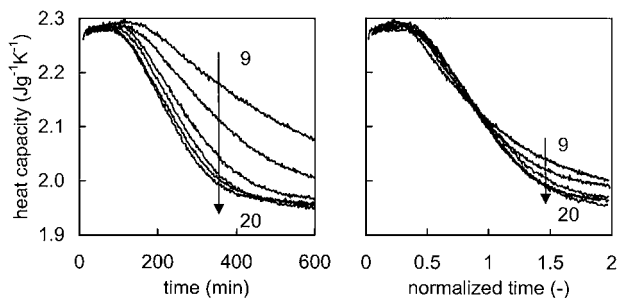


Figure 5 Heat capacity signals (MDSC) during isothermal cure at 35°C for different particle sizes (specific surface indicated in m^2/g).

From Fig. 4 can be concluded that the reaction rate increases with decreasing particle sizes: the heat flow signal is larger for smaller particles and reaches the baseline earlier (reaction is finished sooner).

The heat capacity signals (Fig. 5) on the other hand are not influenced by baseline instabilities and can be used quantitatively over the entire span of the reaction.

The C_p signals are still decreasing long after the heat flow signals reached the baseline. This shows that the reaction is still going on at a very low rate, hence with a very small heat flow released, which disappears in the baseline. The influence of the specific surface of the solid compound on the reaction kinetics can thus be studied quantitatively at 60°C with conventional DSC and at 35°C with DMA and the MDSC C_p signal. The time for onset of vitrification, $t_{0,\text{vit}}$, measured with DMA, can be used as a measure for the reaction rate. Alternatively, the time for reaching a certain stage in the decrease of C_p (for example half of the ΔC_p , $t_{1/2\Delta C_p}$ see Fig. 3) can be used. A good correlation exist between $t_{0,\text{vit}}$ (DMA) and $t_{0,9\Delta C_p}$ (MDSC), see also [2]. For the calculations of $t_{1/2\Delta C_p}$ and $t_{0,9\Delta C_p}$ a total drop of C_p of $0.37 \text{ J} \cdot \text{g}^{-1} \cdot \text{K}^{-1}$ is assumed. This value was not always reached in the experiments, especially for the larger particles, since this would take too long time. The conversions, according to reaction heat, are about 30 and 50% for $t_{0,9\Delta C_p}$ respectively $t_{1/2\Delta C_p}$.

The first step of the reaction evidently involves the break down of the Mk particles. This reaction will probably occur at the surface of the grains. For a reaction taking place at the surface, one expects the reaction rate being dependent on the specific surface. Fig. 6a shows the reaction rate (as maximum height of the heat flow signal) plotted against the specific surface at the beginning of the reaction at 60°C. In Fig. 6b the reaction rate deduced from DMA at 35°C is plotted against the specific surface. It is clear that two reaction regimes are obvious: for small specific surfaces up to $14 \text{ m}^2 \text{ g}^{-1}$ (particle sizes above $2.3 \mu\text{m}$) the reaction rate increases with specific surface (or decreases with particle size), confirming the fact that the rate determining reaction takes place at the surface of the Mk particles.

The further increase of specific surface above $14 \text{ m}^2 \text{ g}^{-1}$ (particles below $2.3 \mu\text{m}$) has no influence on the reaction rate at low conversion (see Fig. 6a and $1/t_{0,\text{vit}}$ in Fig. 6b). This is explained by a two step mechanism: in the first step the solid particles are broken down, generating reactants (building blocks) for the second step. In the second step the building blocks

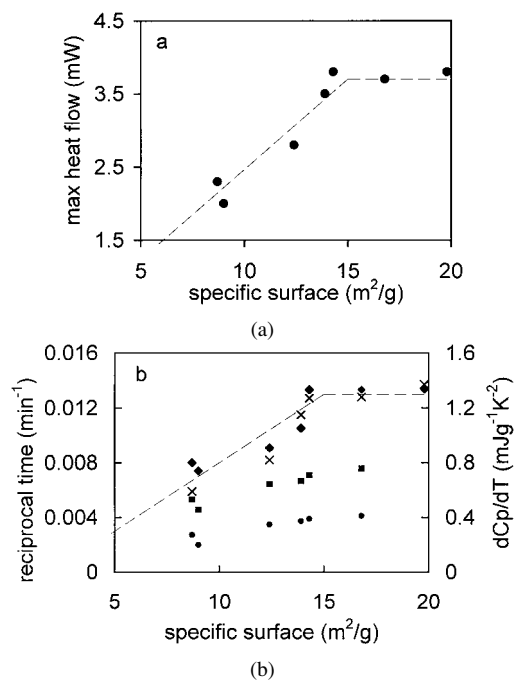


Figure 6 (a) Reaction rate deduced from DSC heat flow signals at the beginning of the reaction at 60°C. The line is drawn as a guide to the eye. (b) Comparison of reaction rates during isothermal cure at 35°C as a function of the specific surface of different Mk fractions. Reaction rates are calculated as reciprocal times (in min⁻¹) from: $t_{0,vit}$, (DMA), \blacklozenge , $t_{0.9\Delta C_p}$, and $t_{1/2\Delta C_p}$, \bullet (MDSC) and as the maximum rate of dC_p/dT , \times .

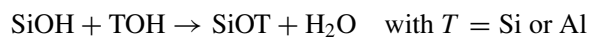
are combined, together with the SiO₄ monomers and oligomers of the silicate solution. The reaction product is the final IPG network structure. From a certain specific surface on, the rate of Mk breakdown becomes comparable to the rate of the network formation and is thus no longer rate determining. A further increase in specific surface will therefore have no or little effect on the global reaction rate.

The C_p signal can also be used for comparing reaction rates, but only for times, longer than the onset of vitrification, thus at a higher conversion, compared to DMA. In Fig. 6b these reaction rates (deduced from the reciprocal times for reaching a certain C_p drop) are plotted against the specific surface. It can be concluded that also at these conversions (where the drop in C_p equals 10% resp. 50%) the reaction rate increases linearly with the specific surface. For specific surfaces above 14 m² g⁻¹, the increase in rate becomes again smaller. Remark that this coincides with the specific surfaces where with DMA (at lower conversion) an invariance of vitrification rate with particle size is observed. Thus beyond the vitrification observed by DMA the reaction rate is still influenced by the particle size. This probably also means that Mk breakdown is not yet finished but continues after the onset of vitrification.

All reaction steps have their own reaction heat. This explains the complexity of the DSC heat flow signal (Figs 2 and 4) which is the sum of the reaction heats of all steps. From the foregoing discussion can be concluded that the initial steep decrease of the heat flow signal observed at least for the smaller particles is linked to the Mk breakdown. The second step, the polymerization, probably starts soon after the initial Mk breakdown with a small reaction rate. This step will become more

important however as the reaction proceeds. This part of the reaction seems to be autocatalytic: the reaction rate increases after the onset of vitrification, at least for the smaller particle sizes. This is probably due to the increasing concentration of building blocks resulting from the breakdown of Mk. The fact that the reaction is not slowed down upon vitrification can be explained by the fact that the reaction occurs in the liquid state (in the remaining silicate) which is entrapped by the forming network. Since the constituents of this liquid phase are small molecules in an aqueous environment no severe mobility restriction occurs, at least not up to $t_{1/2\Delta C_p}$.

The normalized heat capacity curves (Fig. 5, normalized time scale) have about the same shape up to $t_{1/2\Delta C_p}$ indicating that the reaction rates are proportional during the beginning of the reaction. At longer times however, the larger particles react relatively still slower. This can be explained by the hindered mass transport: upon vitrification (already before $t_{1/2\Delta C_p}$) a vitrified network is formed around each shrinking Mk particle. This network grows and restricts (to some extent) the mobility of the remaining reagents in the liquid. On the other hand the low-temperature polymerization includes the exclusion of water according to



The remaining silicate will be diluted during the polymerization, lowering its T_g and enabling mobility till completion of the reaction. The silicate continues to attack the remaining Mk, and the resulting building blocks combine, eventually with monomer and oligomers of the silicate solution, and attach to the existing network.

Evidence for hindered mass transport during reaction of larger particles was already given in previous publications [1]. In a non-isothermal DSC experiment (Fig. 7), a reaction exotherm can be observed between 200 and 300°C, far above the normal reaction exotherm around 100°C. The first exotherm gets smaller while the second exotherm gets larger for Mk fractions with smaller specific surfaces, and it disappears for the largest specific surfaces. From X-ray diffraction patterns and IR (not shown, see [16]) of samples before and after this high temperature exotherm can be concluded that the remaining Mk reacts at this

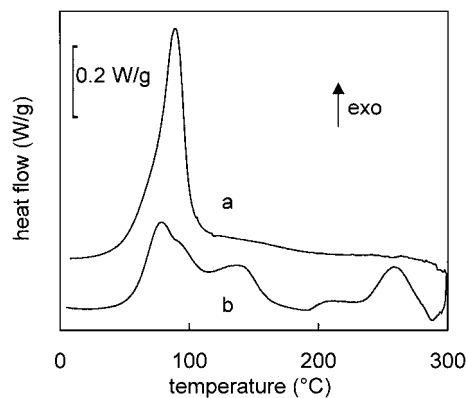


Figure 7 Non-isothermal DSC thermograms of the reaction of (a) fine (20 m²/g) and (b) very coarse particles (coagulations of 200–500 μm).

elevated temperature and pressure with the remaining silicate to form analcyme, $\text{Na}_2\text{O}\cdot\text{Al}_2\text{O}_3\cdot 4\text{SiO}_2\cdot 2\text{H}_2\text{O}$ thus not IPG.

4. Conclusions

The effect of the particle size of metakaolinite on the reaction kinetics of low temperature synthesized inorganic polymer glasses is studied. A characteristic time for the isothermal reaction (onset of vitrification) could be measured with DMA. The influence of particle size on reaction kinetics can also be investigated with MDSC, via the heat flow, but also via the heat capacity, reflecting the vitrification, and via the phase angle. The heat capacity signal can be followed quantitatively during the complete course of the reaction, even if the heat flow signal is too small for quantitative interpretations. It is concluded that the reaction rate increases with decreasing particle size, according to the specific surface. However for specific surfaces above $14\text{ m}^2\text{ g}^{-1}$ this influence becomes small. For the largest particles hindered mass transport occurs during the polymerization.

The DMA and MDSC results indicate that the reaction occurs in at least two steps. In the first step the metakaolinite grains are broken down. In the second step the reaction products of the first reaction combine together with the silicate forming the inorganic polymer network. From the experiments it is also obvious that with MDSC, compared to DMA more information (kinetic and mechanistic) is gained about the reaction. For these measurements, the heat capacity measured with MDSC is the most reliable and useful signal, which can be followed during the complete course of the reaction.

Combining these results with spectroscopic data during the reaction will allow to elucidate the reaction mechanism, and to model the reaction kinetics with a mechanistic approach.

References

1. H. RAHIER, B. VAN MELE, M. BIESEMANS, J. WASTIELS and X. WU, *J. Mater. Sci.* **31** (1996) 71.
2. H. RAHIER, B. VAN MELE and J. WASTIELS, *ibid.* **31** (1996) 80.
3. H. RAHIER, W. SIMONS, B. VAN MELE and M. BIESEMANS, *ibid.* **32** (1997) 2237.
4. G. VAN ASSCHE, A. VAN HEMELRIJCK, H. RAHIER and B. VAN MELE, *Thermochim. Acta* **268** (1995) 121.
5. S. SWIER, G. VAN ASSCHE, A. VAN HEMELRIJCK, H. RAHIER, E. VERDONCK and B. VAN MELE, *J. Thermal Anal.* **54** (1998) 585.
6. H. RAHIER, B. WULLAERT and B. VAN MELE, *J. Therm. Anal. Cal.* **62** (2000) 417.
7. G. ENGELHARDT and D. MICHEL, "High Resolution Solid State NMR of Silicates and Zeolites" (J. Wiley, Chichester, 1987).
8. R. K. HARRIS and C. T. G. KNIGHT, *J. Chem. Soc., Faraday Trans. 2* **79** (1983) 1525.
9. M. READING, *Trends Polymer Science* **1** (1993) 248.
10. P. DE MEUTER, H. RAHIER and B. VAN MELE, *Int. J. Pharm.* **192** (1999) 77.
11. P. DE MEUTER, J. AMELRIJCKX, H. RAHIER and B. VAN MELE, *J. Pol. Science B* **37** (1999) 2881.
12. K. DE CLERCK, H. RAHIER, B. VAN MELE and P. KIEKENS, *J. Appl. Pol. Science* accepted.
13. *Idem.*, *ibid.* accepted.
14. F. ROUQUEROL, J. ROUQUEROL and K. SING, "Adsorption by Powders and Porous Solids" (Academic Press, San Diego, 1999) p. 166.
15. S. J. GEGG, *Chem. & Ind.* **611**, 1968.
16. H. RAHIER and B. VAN MELE, to be published.

Received 26 September 2001
and accepted 18 April 2003